Indian Journal of Science and Technology, Vol 9(4), DOI: 10.17485/ijst/2016/v9i4/72038, January 2016
ISSN (Print) : 0974-6846
ISSN (Online) : 0974-5645

Performance Comparison of Line-Start Permanent Magnet Synchronous Motors with Interior and Surface Rotor Magnets

Cosmas U. Ogbuka*, Cajethan M. Nwosu and Marcel U. Agu

Department of Electrical Engineering, University of Nigeria, Nsukka Enugu State, Nigeria;
cosmas.ogbuka@unn.edu.ng, cajethan.nwosu@unn.edu.ng, marcel.agu@unn.edu.ng

Abstract

Objectives: The aim is to undertake a comprehensive comparison of the dynamic and steady state performance of Permanent Magnet Synchronous Motors (PMSM) with interior and surface rotor magnets for line-start operation. **Methods/Analysis:** The dynamic model equations of the PMSM, with damper windings, are utilized for dynamic studies. Two typical loading scenarios are examined: Step and ramp loading. Emphasis was on the synchronization and load-withstand capabilities of the two motor classes. Also, the steady state torque performance was compared using the torque/torque angle relationship. **Findings:** The interior permanent magnet synchronous motor (IPMSM) showed superior asynchronous performance under no load, attaining faster synchronism compared to the Surface Permanent Magnet Synchronous Motor (SPMSM). With step load of 10Nm at 2 seconds the combined effect of the excitation and the reluctance torque forced the IPMSM to pull into synchronism faster than the SPMSM which lacks saliency. The ability of the motors to withstand gradual load increase, in the synchronous mode, was examined using ramp loading starting from zero at 2seconds. SPMSM lost synchronism at 12seconds under 11Nm load while the IPMSM sustained synchronism until 41seconds under 40Nm load. This clearly suggests that the IPMSM has superior load-withstand capability. The superiority is further buttressed with the steady state torque analysis where airgap torque in IPMSM is enhanced by the reluctance torque within 90º to 180º torque angle. **Applications:** The findings of this research will serve as guide in taking logical decisions in the design and operation of permanent magnet synchronous motors to achieve desired objectives in specific applications.

Keywords: Airgap Torque, Damper Winding, IPMSM, PMSM, Reluctance Torque, SPMSM, saliency

1. Introduction

The recent concentration of research efforts in the design, analysis and control of the Permanent Magnet Synchronous Motors (PMSM) is justified because for the same output power, PMSM offer performance enhancement over the conventional induction and synchronous motors in terms of power factor, efficiency, power density and torque-to-inertia ratio[1–8]. The performance superiority of the PMSM over the traditional induction and wound rotor synchronous motors have also been reported in[9–12]. Emphasis in electric drives in now on energy saving[13] and PMSM is a competitive option. The PMSM has also been favoured, when compared to induction motor, for line start operation, variable speed operation and in the field of semi-hermetic drives as respectively reported in[14–16].

A key issue of interest in the design of PMSM is the nature of the permanent magnet material. The properties of the permanent magnet material will affect directly the performance of the PMSM. Neodymium Iron-Boron $Nd_2Fe_{14}B$ (Neodymium Iron Boron) is presently the best choice due its superior B-H characteristics[17]. The problem of high cost and limited supply makes supply unpredictable and researches are presently on to enhance on ferrites to achieve competitive power density and efficiency of the rare-earth PMSM[18–20].

Interior Permanent Magnet Synchronous Motor (IPMSM) and Surface Permanent Magnet Synchronous

*Author for correspondence

Motor (SPMSM) are the two major classes of PMSM based on the placement of the rotor permanent magnets. Surface-mounted PM motors have each of the permanent magnets mounted on the surface of the rotor, making it easy to build, and specially skewed poles are easily magnetized on this surface mounted type to minimize cogging torque. This configuration is used for low speed applications because of the limitation that the magnets will fly apart during high-speed operations. These motors are considered to have insignificant saliency, thus having practically equal inductances in both the q and d axes. The ratio between the quadrature and direct axis inductances is unity (i.e., $L_d = L_q$). Figure 1 shows the placement of rotor magnets in SPMSM[21,22].

IPMSM on the other hand, have rotors with interior mounted permanent magnets as shown in Figure 2. Because of the internal positioning of the rotor magnets, it is good for high-speed operation. These motors have saliency with q-axis inductance greater than the d-axis inductance ($L_q > L_d$). The magnets are very well protected against centrifugal forces[23]. Several other classifications of PMSM, based on the placement of rotor magnets, are discussed in[24]. Special rotor designs have continued to evolve to satisfy specific operational requirements.

The difference in rotor magnet placement affords the two PMSM configurations different performance characteristics. In the present study, a comprehensive dynamic and steady state comparison is made between the IPMSM and the SPMSM, of the same 4hp rating, for line-start operation. Specifically, the run-up characteristics will be observed from rest to synchronous speed affording the opportunity to study and compare the motors within the asynchronous speed range under no load. This will be followed by two loading scenarios; 1. Step loading and 2. Ramp loading to establish the load withstand capabilities of the two motors. Finally, the steady state torque characteristics of the two motors would be examined to verify the effect of the reluctance torque component associated

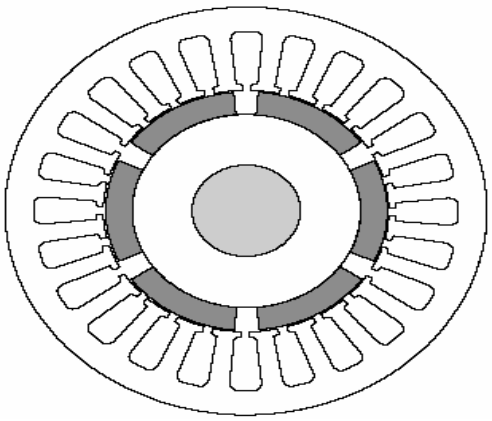

Figure 1. SPMSM rotor assembly.

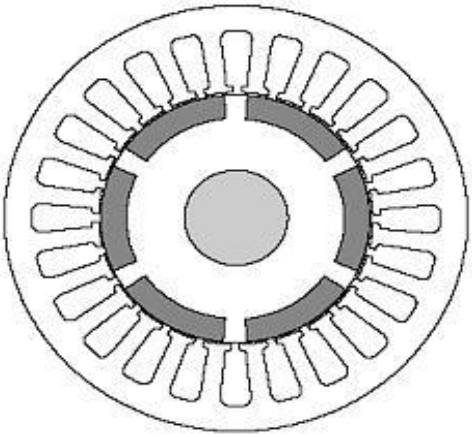

Figure 2. IPMSM rotor assembly.

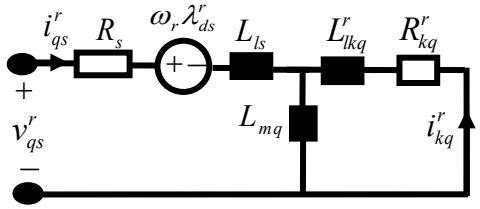

Figure 3 . Q-axis equivalent circuit.

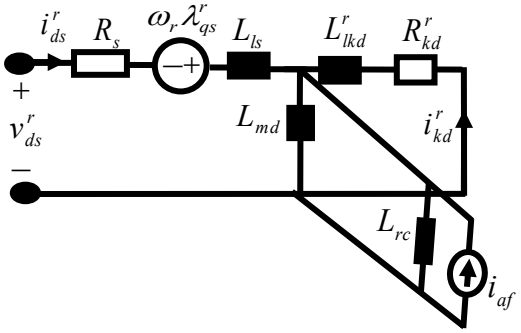

Figure 4. D-axis equivalent circuit.

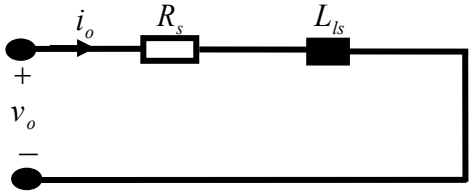

Figure 5. Zero-sequence equivalent circuit.

with IPMSM as the torque angle varies. MATLAB will be used as the software tool for this research.

2. Line-Start Dynamic Model of PMSM

Although the industrial use of inverters for variable speed drives is widespread, constant speed line-start operation of PMSM is still dominant in medium, low, and fractional horsepower applications. The PMSM being inheritably non self starting, damper windings are employed to run the machine up to speed on induction motor action with the motor pulling into synchronism by a combination of the reluctance and synchronous motor torques provided by the magnet. During the start-up, the magnet exerts a braking torque that opposes the induction-motor-type torque provided by the damper windings. The torque provided by the damper windings must therefore overcome this magnet braking torque in addition to the load and friction, to run-up the motor successfully.

The following parameters are defined: v^r_{qs} = stator q-axis voltage, v^r_{ds} = stator d-axis voltage, v_o = zero sequence voltage, i^r_{qs} = stator q-axis current, i^r_{ds} = stator d-axis current, i_o = zero sequence current, R_s = stator resistance, ω_r = rotor speed, λ^r_{ds} = stator d-axis flux linkage, λ^r_{qs} = stator q-axis flux linkage, L_{mq} = q-axis magnetizing inductance, L_{md} = d-axis magnetizing inductance, L_{ls} = stator leakage inductance, $L_d = L_{ls} + L_{md}$, $L_q = L_{ls} + L_{mq}$, L^r_{lkq} = q-axis damper winding inductance, L^r_{lkd} = d-axis damper winding inductance, R^r_{kq} = q-axis damper winding resistance, R^r_{kd} = d-axis damper winding inductance, i^r_{kq} = q-axis damper winding current, i^r_{kd} = d-axis damper winding current, $\lambda_{af} = L_{md} i_{af}$ = magnetic flux linkage, J = moment of inertia, B = frictional coefficient.

The equivalent qd0 circuit of a line-start permanent magnet synchronous motor with the reference frame fixed in the rotor is shown below.

The corresponding qd0 dynamic equations for the motor are summarized below.

$$v^r_{qs} = R_s i^r_{qs} + p\lambda^r_{qs} + \omega_r \lambda^r_{ds} \tag{1}$$

$$v^r_{ds} = R_s i^r_{ds} + p\lambda^r_{ds} - \omega_r \lambda^r_{qs} \tag{2}$$

$$v_0 = R_s i_0 + p\lambda_o \tag{3}$$

$$0 = R^r_{kd} i^r_{kd} + p\lambda^r_{kd} \tag{4}$$

$$0 = R^r_{kq} i^r_{kq} + p\lambda^r_{kq} \tag{5}$$

Flux linkages are defined as follows:

$$\lambda^r_{qs} = L_q i^r_{qs} + L_{mq} i^r_{kq} \tag{6}$$

$$\lambda^r_{ds} = L_d i^r_{ds} + L_{md} i^r_{kd} + \lambda^r_{af} \tag{7}$$

$$\lambda^r_{af} = L_{md} i^r_{af} \tag{8}$$

$$\lambda_0 = L_{ls} i_0 \tag{9}$$

$$\lambda^r_{kq} = L_{mq} i^r_{qs} + L^r_{kq} i^r_{kq} \tag{10}$$

$$\lambda^r_{kd} = L_{md} i^r_{ds} + L^r_{kd} i^r_{kd} + L_{md} i^r_{af} \tag{11}$$

The developed electromagnetic torque is derived as

$$T_e = \frac{3}{2}\frac{P}{2}(\lambda_{af} i^r_{qs}) + \frac{3}{2}\frac{P}{2}(L_d - L_q) i^r_{ds} i^r_{qs} + \\ + \frac{3}{2}\frac{P}{2}(L_{md} i^r_{kd} i^r_{qs} - L_{mq} i^r_{kq} i^r_{ds}) \tag{12}$$

The first, second and third components of T_e are the excitation torque, reluctance torque and induction torque respectively. The damper windings are practically disengaged as soon as the rotor reaches synchronous speed. Equations (12) reduces to

$$T_e = \frac{3}{2}\frac{P}{2}[\lambda_{af} + (L_d - L_q) i^r_{ds}] i^r_{qs} \tag{13}$$

The rotor dynamics is governed by the following set of relationships

$$T_e = J\frac{d\omega_r}{dt} + T_L + B\omega_r \tag{14}$$

$$P\omega_r = \frac{1}{J}(T_e - T_L - B\omega_r) \tag{15}$$

$$P\theta_r = \omega_r \tag{16}$$

2.1 Steady State Torque Analysis

Steady state torque characteristics of the PMSM highlights the relationship between the torque components and the torque angle δ. Assume the following set of balanced polyphase current as the input to the PMSM:

$$I_{qs} = I_m \sin(\omega_r t + \delta) \tag{17}$$

$$I_{ds} = I_m \cos(\omega_r t + \delta) \tag{18}$$

Where δ is the angle between the rotor flux λ_{af} and stator current phases and known as the torque angle since it determines the steady state torque.

Using the inverse transformation ratio $[T^r]^{-1}$,

$$[T^r]^{-1} = \begin{bmatrix} \cos\theta_r & -\sin\theta_r \\ \sin\theta_r & \cos\theta_r \end{bmatrix} \quad (19)$$

The steady state stator current components in the rotor reference frame as shown in Figure 6 are:

$$I_{qs}^r = I_m \sin\delta \quad (20)$$

$$I_{ds}^r = I_m \cos\delta \quad (21)$$

Based on the Figure 6, at steady state, the airgap torque equation (i.e., Equation (13)) becomes

$$T_e = \frac{3}{2}\frac{P}{2}[\lambda_{af} + (L_d - L_q)I_{ds}^r]I_{qs}^r \quad (22)$$

Substituting Equations 20 and 21 into Equation 22

$$T_e = \frac{3}{2}\frac{P}{2}[\lambda_{af} I_m \sin\delta + \frac{1}{2}(L_d - L_q)I_m^2 \sin 2\delta] \quad (23)$$

The torque angle δ directly influences the air-gap torque T_e. The torque expression contains two components; the synchronous torque (excitation torque) $T_{es} = \frac{3}{2}\frac{P}{2}\lambda_{af} I_m \sin\delta$ which is due to the interaction of the rotor magnetic field and the q axis stator current and the reluctance torque $T_{er} = \frac{3}{2}\frac{P}{2}\frac{1}{2}(L_d - L_q)I_m \sin 2\delta$ due to reluctance variation.

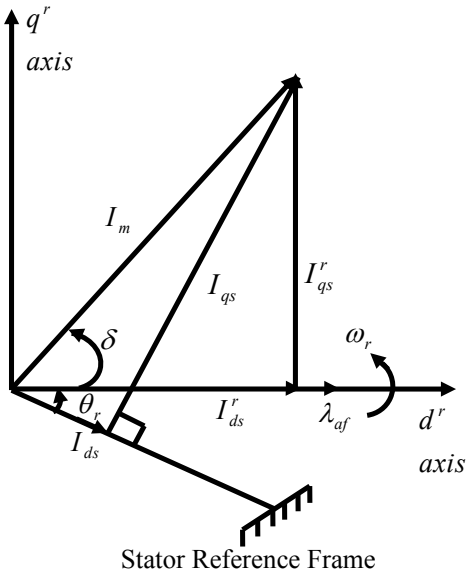

Figure 6. Stator input current phasor diagram.

3. Results and Analysis

The parameters of the interior and surface PMSM are shown in the Table 1. The two motors are rated 4Hp and operated at the rated voltage of 220V and 50Hz frequency. The results of the dynamic and steady state studies are presented in the plots below.

3.1 Dynamic Comparison

The dynamic characteristics of the two motors are investigated under two scenarios. The first scenario allows the motor to run-up to synchronous speed before a step load of 10Nm is applied at 2 seconds. The load is then removed suddenly at 3 seconds. It is seen from Figure 7 that the IPMSM synchronises faster than the SPMSM. This faster synchronisation of IPMSM is also observed during speed recovery from sudden gain or loss of load as shown in Figure 8.

From Figures 9 and 10, the airgap (electromagnetic) torque for the IPMSM is greater than that of the SPMSM

Table 1. PMSM parameters

Motor Parameter		IPMSM	SPMSM
Rated Power	Hp	4	4
Frequency	Hz	50	50
Rated Phase Voltage	$V(Volts)$	220	220
Stator Resistance	$R_s(\Omega)$	0.0906	0.2306
Magnetising Flux Linkage	$\lambda_{af}(weber.turn)$	0.1546	0.1546
Stator Leakage Inductance	$L_{ls}(H)$	0.0016	0.0028
d-axis Magnetizing Inductance	$L_{md}(H)$	0.0206	0.0441
q-axis Magnetizing Inductance	$L_{mq}(H)$	0.0441	0.0441
Moment of Inertia	$J(Kgm^2)$	0.4200	0.4200
No. of Poles	P	6	6
Damper Winding Parameters			
d-axis Damper Leakage Inductance	$L_{lkd}^r(H)$	0.0057	
q-axis Damper Leakage Inductance	$L_{lkq}^r(H)$	0.0057	
d-axis Damper Resistance	$R_{kd}^r(\Omega)$	0.7324	
q-axis Damper Resistance	$R_{kq}^r(\Omega)$	1.6230	

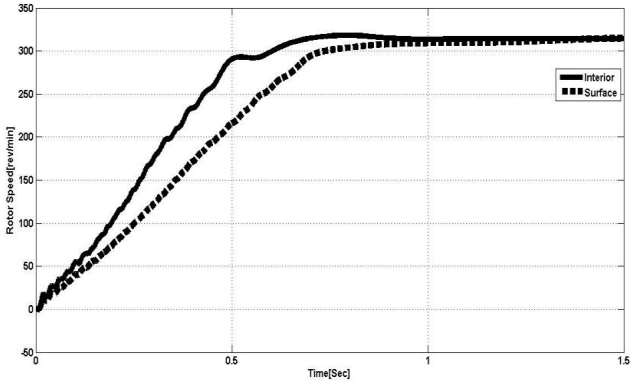

Figure 7. Transient speed at no load.

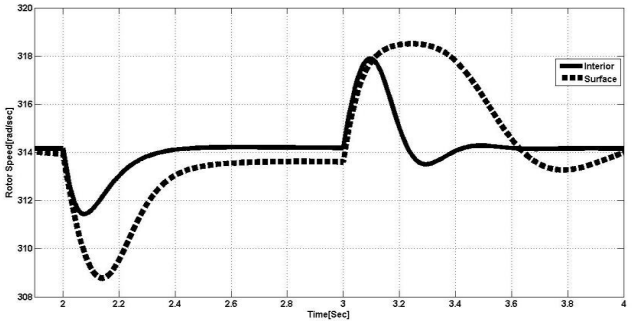

Figure 8. Speed dynamics due to sudden load changes.

below synchronous speed. This region is the asynchronous region. Upon initial attainment of synchronous speed, a combination of the excitation and the reluctance torque enables the IPMSM to quickly synchronise as shown in Figure 10. The direct proportionality between stator current and airgap (electromagnetic) torque explains the behaviour of the stator current in response to electromagnetic torque as shown in Figures 11 and 12.

The second loading scenario compares the load-withstand capabilities of the two motors as shown in Figures 13 and 14. Ramp loading is applied at 2 seconds (after synchronisation). Unlike the SPMSM that lost synchronism at 12seconds under 11Nm load, the IPMSM sustained synchronism until 41 Seconds absorbing as much as 40 Nm load torque before lose of synchronism.

3.2 Steady State Torque Comparison

For the steady state torque comparison, the airgap torque and its components are plotted with a stator current magnitude of 4A for the IPMSM as shown in Figure 15. It is noted that the peak of the airgap torque is at angle greater than 90°. The reluctance torque enhances the airgap torque only in the torque angle range from

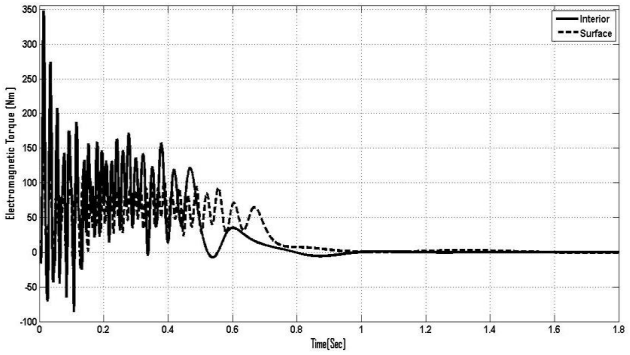

Figure 9. Airgap torque dynamics at no load.

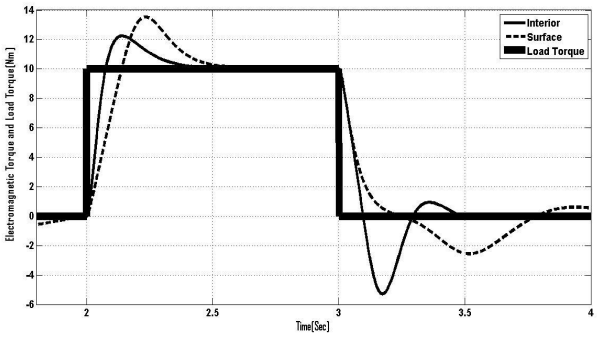

Figure 10. Torque dynamics due to sudden load changes.

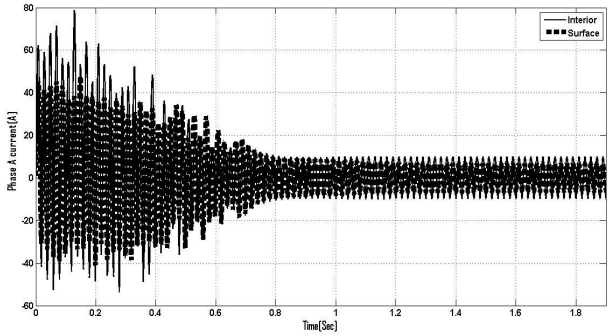

Figure 11. Stator current transient at no load.

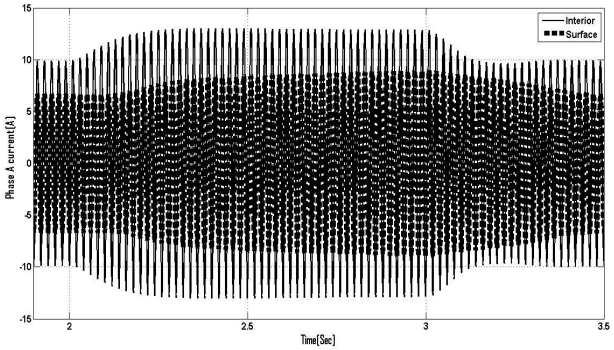

Figure 12. Stator current dynamics due to sudden load changes.

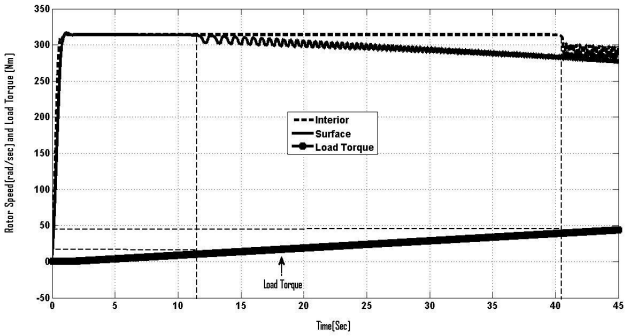

Figure 13. Speed dynamics with ramp loading.

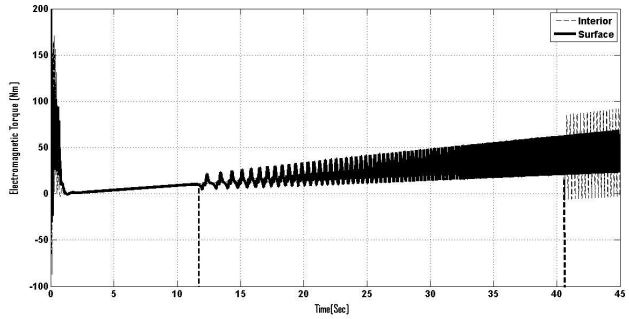

Figure 14. Torque dynamics with ramp loading.

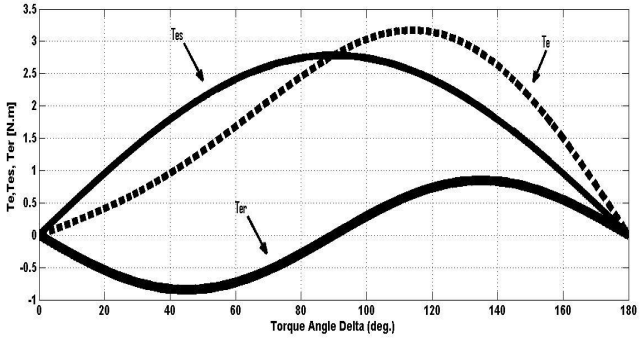

Figure 15. Steady state torque components of IPMSM.

90° to 180°; thus the preferred torque angle range of operation is between 90° to 180°. Figure 16 compares the airgap torque for the IPMSM and the SPMSM. The enhancement offered by the reluctance torque at torque range between 90° to 180° is clearly evident and this makes the peak of the torque curve to occur at angle above 90° for the IPMSM. The SPMSM has airgap torque equal to the synchronous (excitation) torque. Being a pure sinusoid, the peak of the steady state torque occurs at torque angle of 90°.

4. Conclusion

This paper has, objectively, compared the dynamic and the steady state performance of the IPMSM and the SPMSM for line-start operation under two dominant loading scenarios. Emphasis was on the run-up characteristics under no load and the response of the motors to loading upon attainment of synchronism as well as the steady state torque characteristics.

The ability of the motors to withstand gradual load increase was examined using ramp loading. Once again, while the SPMSM lost synchronism at 12seconds under 11Nm load, the IPMSM sustained synchronism until 41seconds absorbing as much as 40Nm load torque before lose of synchronism. The clearly suggests that the IPMSM has superior load-withstand capability compared to the SPMSM.

The outcome of this research will serve as a guide to operation engineers in taking logical decisions in the selection of machines to execute specific assignment. The design engineers also will find the work useful in the appropriate selection of design parameters in designing PMSM to satisfy specific application area.

5. References

1. Selvam NP, Rajasekaran V, Jayanthi N. Performance analysis of DTC-CSI fed IPMSM drive at very low speed with stator resistance compensation. Indian Journal of Science and Technology. 2015; 8(18):1–9.
2. Cahil DPM, Adkins B. The permanent magnet synchronous motor. Proceedings of the IEEE–Part A: Power Engineering. 1962; 109A(38):483–91.
3. Weschta A. Design considerations and performance of brushless permanent magnet servo motors. Conference Record IAS-Annual Meeting; San Francisco. 1982. p. 469–75.
4. Pfaff G, Weschata A, Wick A. Design and experimental results of a brushless AC servo drive. IEEE Transactions on Industry Applications. 1984; IA-20(4):814–21.
5. Demerdash NA, Nehl TW. Dynamic modelling of brushless DC motors for aerospace actuation. IEEE Transactions on Aerospace and Electronic Systems. 1980; AES-16(6):810–8.
6. Miller RH, Nehl TW, Demerdash NA, Overton BP, Ford CJ. An electronically controlled permanent magnet synchronous machine conditioner system for electric passenger vehicle propulsion. Conference Record IAS-Annual Meeting; San Francisco. 1982. p. 506–10.
7. Maggetto G, Sneyers B, VanEck JL. Permanent magnet motors used for traction purposes. Proc of Motorcon Conference; Oxnard, California. 1982. p. 61–8.

8. Homer GR, Lacey RJ. High performance of brushless pm motors for robotics and actuator applications. Proceedings 1st European Conference on Electrical Drives/Motor/ Control. 1982. p. 91–9.
9. Pillay P, Krishnan R. Modeling, simulation, and analysis of permanent-magnet motor drives. I. The permanent-magnet synchronous motor drive. IEEE Transactions on Industry Applications. 1989; 25(2):265–73.
10. Ong CM. Dynamic simulation of electric machinery using MATLAB and simulink. Upper Saddle River, New Jessy: PTR; 1997. p. 309–40.
11. Abdel-Kader FM, Osheba SM. Performance analysis of permanent magnet synchronous motors. Part 1: Dynamic performance. Transactions on Energy Conversion. 1990; 5(2):611–4.
12. Cahill DP, Adkin M. The permanent magnet synchronous motor. Proceedings of the IEE-Part A: Power Engineering. 1962; 109A(48):483–91.
13. Ravindran M, Kirubakaran V. Analysis of energy saving methods in different motors for consumer applications. Indian Journal of Science and Technology. 2015; 8(S8):297–305.
14. Marcic T, Stumberger B, Stumberger G, Hadziselimovic M, Virtic P, Dolinar D. Line-starting three- and single-phase interior permanent magnet synchronous motors-direct comparison to induction motors. IEEE Transactions on Magnetics. 2008; 44(11):4413–6.
15. Marcic T, Stumberger B, Stumberger G. Comparison of induction motor and line-start IPM synchronous motor performance in a variable-speed drive. IEEE Transactions on Industry Applications. 2012; 48(6):2341–52.
16. Stumberger B, Marcic T, Hadziselimovic M. Direct comparison of induction motor and line-start IPM synchronous motor characteristics for semi-hermetic compressor drives. IEEE Transactions on Industry Applications. 2012; 48(6):2310–21.
17. Krishnan R. Permanent magnet synchronous and brushless DC motor drives. Boca Roton: CRC Press Taylor and Francis Group; 2009.
18. Obata M, Morimoto S, Sanada M, Inoue Y. Performance of pmasynrm with ferrite magnets for EV/HEV applications considering productivity. IEEE Transactions on Industry ApplIcations. 2013; 50(4):2427–35.
19. Sanada M, Inoue Y, Morimoto S. Structure and characteristics of high-performance pmasynrm with ferrite magnets. Transactions on Industry Applications. 2014; 187(1):42–50.
20. Morimoto S, Ooi S, Inoue Y, Sanada M. Experimental evaluation of a rare-earth-free pmasynrm with ferrite magnets for automotive applications. IEEE Transactions on Industrial Electronics. 2014; 61(10):5749–56.
21. Krishnan R. Electric motor drives modeling, analysis, and control. Pearson Education; 2001.
22. Aydin M. Axial flux mounted permanent magnet disk motors for smooth torque traction drive application. Madison: University of Wisconsin; 2004. p. 1–11.
23. Jahns TM. Interior permanent-magnet synchronous motors for adjustable speed drives. IEEE Transactions on Industry Applications. 1986; 22(4):738–46.
24. Qinghua L. Analysis, design and control of permanent magnet synchronous motors for wide-speed operation. Singapore: National University of Singapore. 2005. p. 1–40.